2019 EAGE ANNUAL
81ST CONFERENCE + EXHIBITION
LONDON | THE UNITED KINGDOM

We_R01_16

Specular Imaging of Converted Wave Data and its AVO Impact

A. JafarGandomi[1], O. Bukola[1], R. Refaat[1]*, H. Hoeber[1]

[1] CGG

Summary

In principle, high quality pre-stack converted wave (PS) data can provide valuable complementary information to conventional P wave (PP) data to highlight seismic amplitude anomalies in areas with complex imaging problems such as steeply dipping structures and obscured areas. However, in practice, we often find that PS images are noisier than the corresponding PP images. In addition, the amplitude versus offset (AVO) behaviour of PS gathers is generally poor and joint PP-PS AVO analysis is a struggle.

In this paper, we propose to employ specular imaging for converted waves. Benefits of specular imaging with dip-angle migration have been widely shown both for 3D imaging and 4D monitoring of P wave data. Here we apply the specular imaging method to an ocean-bottom cable (OBC) dataset from the North Sea to enhance the PS images. We show that, by selection of specular energy in the dip-angle domain, PS images are significantly less noisy and migration artefacts are reduced. As a result, the AVO compliance of specular migrated gathers is significantly enhanced.

Introduction

In principle, high quality pre-stack converted wave (PS) data can provide valuable complementary information to conventional P wave (PP) data to highlight amplitude anomalies in areas with complex imaging problems such as steeply dipping structures and obscured areas. However, in practice, we often find that PS images are noisier than the corresponding PP images. In addition, the amplitude versus offset (AVO) behaviour of PS gathers is generally poor and joint PP-PS AVO analysis is a struggle.

In this paper, we propose to employ specular imaging for converted PS waves. Benefits of specular imaging with dip-angle migration have been widely shown (Audebert et al., 2002; Tabti et al., 2004; JafarGandomi et al., 2018) both for 3D imaging and 4D monitoring of P wave data. Here we apply the specular imaging method to an ocean-bottom cable (OBC) dataset from the North Sea to enhance the PS images. We show that, by selection of specular energy in the dip-angle domain, PS images are significantly less noisy and migration artefacts are reduced. As a result, the AVO compliance of specular migrated PS gathers is significantly enhanced.

Analysis of the Fresnel zone for PS specular imaging

Approximating the size of Fresnel zone radius is key in specular imaging. We define the Fresnel zone radius in the dip-angle domain as

$$\Delta\theta = acos\left(\frac{z}{z+\lambda/4}\right), \quad (1)$$

where $\Delta\theta$ is the half-extent of the Fresnel zone in terms of angle, z is depth (m) and λ stands for wavelength (m). In contrast to the offset-depth domain, where the radius of the Fresnel zone increases with depth (Figure 1a), the extent of the Fresnel zone in angle (Equation 1) shrinks with depth for a fixed wavelength (Figure 1b). In general, as the S-wavelength is shorter than that of P-waves, the corresponding Fresnel zone radius is also smaller for S-waves. Eaton (1991) derives expressions for the Fresnel zone radii of the P wave (F_{PP}) and the converted wave (F_{PS}). For a flat reflector with fixed depth and frequency, they are related to the ratio of P- and S-wave velocities Vp/Vs. Based on Eaton's results, we derive the following relationship between the two Fresnel zone radii and the P- and S-wave velocities:

$$\frac{F_{PS}}{F_{PP}} = \sqrt{\frac{2V_S}{V_P+V_S}}. \quad (2)$$

Figure 1c shows the variation of this ratio as a function of Vp/Vs values. Increasing Vp/Vs leads to smaller converted wave Fresnel zones relative to the PP waves; for a typical Vp/Vs of 2.0, the ratio of Fresnel zones is around 0.8. We use the offset and frequency dependency of the size of the Fresnel zone to isolate specular energy in the dip-angle domain.

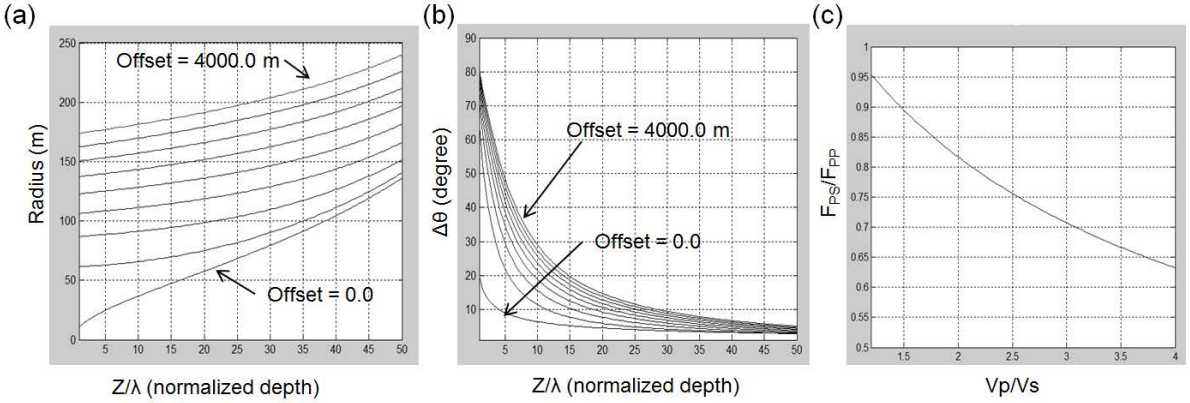

Figure 1 *(a) Variation of radius of Fresnel zone with respect to normalized depth, (b) variation of Fresnel zone half-extent in angle with respect to normalized depth, and (c) variation of Fresnel zone radii F_{PS}/F_{PP} with respect to Vp/Vs.*

The difference between the PP and PS wave Fresnel zones implies that, with the same level of un-cancelled noise for both PP and PS data, the migrated image and gathers for PS will have worse amplitude deficiency and noise level. Equation 2 also implies greater susceptibility of PS images to this effect for geological formations with higher Vp/Vs values.

The Specular Imaging Method

For specular imaging we first generate dip-angle gathers using converted-wave Kirchhoff pre-stack depth migration (PSDM). We then filter the common dip-angle sub-volumes in the wavenumber domain to attenuate non-specular energy outside of the Fresnel zone. In the wavenumber domain we define a tapered mask, centred on the nominal dip-angle of the corresponding migrated sub-volume, whose width is defined by the Fresnel zone. Figure 2 shows an example of a migrated crossline of a North Sea dataset with a dip-angle of 20 degrees before and after applying the specular mask. With this approach, genuine geological events with conflicting dips are preserved, as each event is treated independently within its own corresponding dip-angle sub-volume.

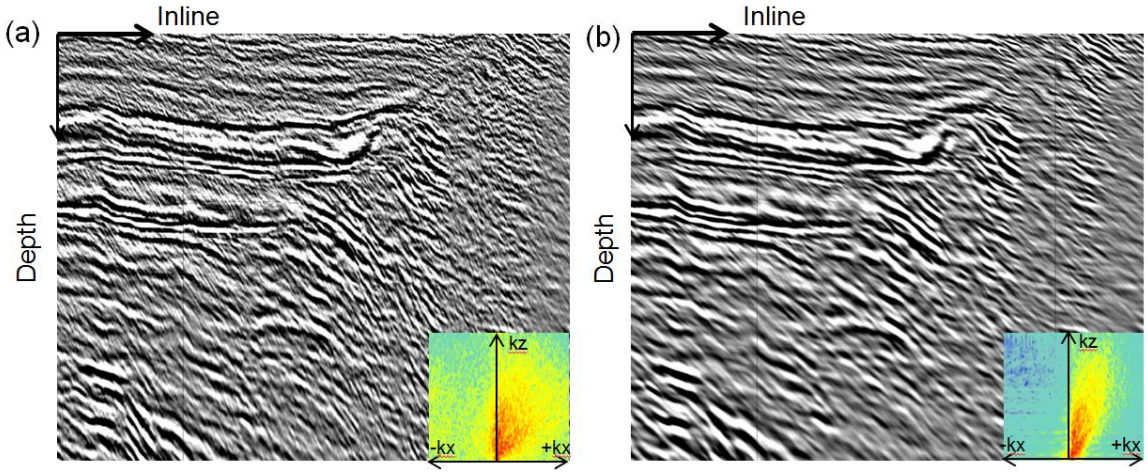

Figure 2 *Migrated common dip-angle (20°) PS images (a) before and (b) after applying the specular mask in the wavenumber domain. Note that the dip may be out of plane.*

A North Sea data example

The developed PS specular imaging approach is applied to an OBC dataset acquired over the Mungo field in the UK Continental Shelf (UKCS) operated by BP in partnership with Zennor Petroleum. Mungo is a large oilfield with a small gas cap. The reservoir is defined by the salt diapir structure, characterized by an extensive oil column in the draped Palaeocene sandstone overlaying the potential, secondary, Cretaceous chalk reservoir. There is a possibility that sediment rafts may be within the salt body. Deeper, pre-salt targets are also considered. High sand/shale shear impedance contrast is expected, suggesting good reservoir potential.

The main challenges are steep reservoir dips (~40-65 degrees) reaching 85 degrees in the South West, structural complexity, and uncertainty in stratigraphic interpretation of the Top Sele (reservoir), Top Chalk and Top Salt at the flanks of the salt body, as well as illumination and the inability to use AVO in the areas of steep dips. The OBC data were acquired with a receiver station spacing of 25 m in the Western part and 50 m in the Eastern part of the data, a cable interval of 400 m, shotpoint interval of 50 m and shotline separation of 100 m. In summary, PS data processing consists of de-noising, static corrections, de-multiple, regularisation and Kirchhoff PSDM. The Vs model was built using a combination of surface wave inversion, full waveform inversion and converted wave tomography.

Figure 3 shows the impact of specular imaging on substack images corresponding to near (0-15 degrees) and far (30-45 degrees) incidence angles. The converted wave images are all stretched to PP time. Note that all of the following images for conventional and specular imaging are raw migration products without any post-migration processing. The specular PS images are significantly less noisy

and migration artefacts are suppressed, especially on the steeply dipping flanks of the salt diaper and for the near-angle stack.

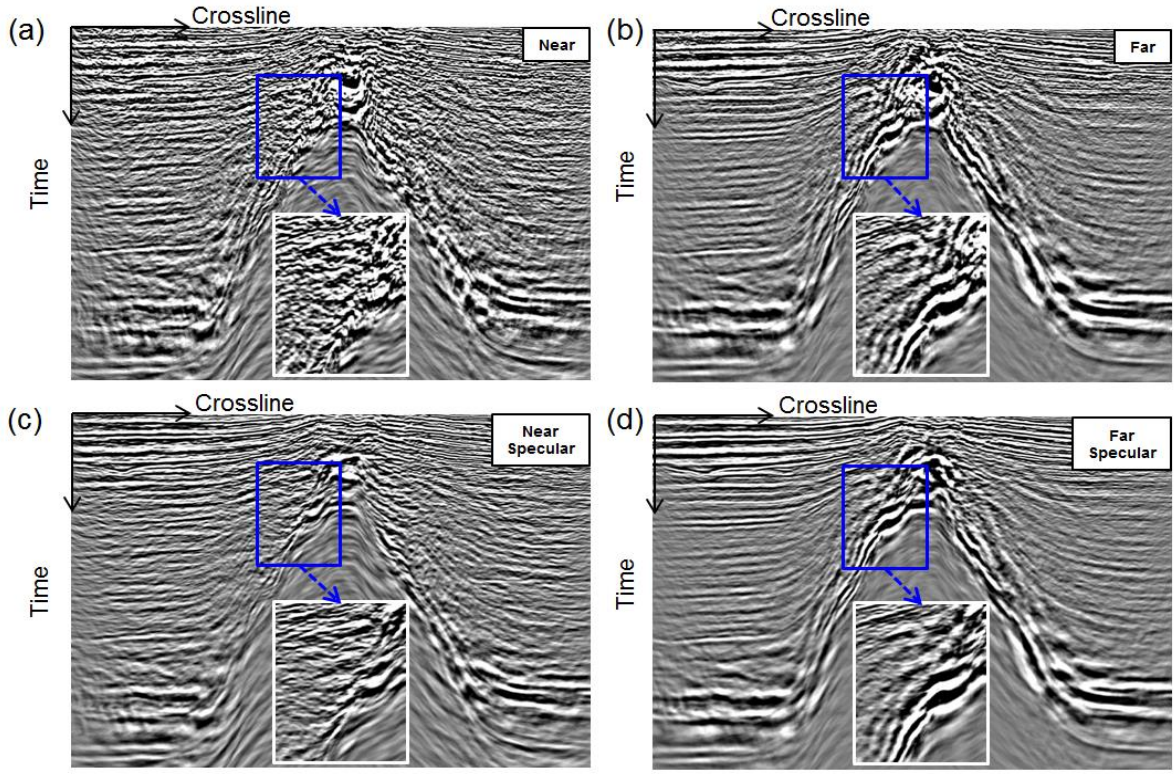

Figure 3 *Migrated near- and far-angle stacks for conventional (a & b) and specular (c & d)* PS *Kirchhoff PSDM.*

Figure 4 shows the impact of the noise reduction for PS AVO behaviour. The variation of RMS amplitudes versus scattering angle with specular imaging (curves shown on top of the gathers in Figure 4b) follow the expected PS AVO response, where amplitudes are weaker at the near and far angles, compared to the mid angles. Without specular imaging (Figure 4a), this behaviour appears masked by noise, particularly for the near angles; this may well be due to the Fresnel zone variation shown in Figure 1. With specular imaging, the estimated gradient from a two-term fit of the near angles is significantly cleaner and has weaker amplitude, as is expected from PS AVO (Figure 4d). We expect this cleaner gradient to make AVO interpretation easier on the final processed gathers, especially around the flanks of the salt diapir where migration artefacts obscure the geological events. The AVO fit residuals (difference between data and AVO models) are significantly reduced with specular imaging, which is a clear indication of improved AVO compliance of the PS data (Figures 4e & 4f).

Conclusions

We have shown that applying dip-angle domain specular imaging to converted PS data significantly reduces migration artefacts and noise. Analysis of the Fresnel zone for PS data shows that the near offsets have a much smaller specular radius than the far offsets. This has a noticeable impact on the amplitude of the near offsets, which leads to significant improvement in the AVO behaviour of migrated PS gathers. In effect, the expected AVO behaviour was masked by migration noise in conventional PS imaging. Further work will investigate the impact of the PS and PP specular imaging on event registration, and the possibility of joint AVO fitting or inversion.

Acknowledgements

We thank BP and Zennor Petroleum for show rights of the North Sea dataset. Thanks are due to everyone in the CGG Crawley centre involved in the processing and imaging of the PS data.

References

Audebert, F., Froidevaux, P., Rakotoarisoa, H. and Svay-Lucas, J. [2002] Insights into migration in the angle domain. In 72th SEG Technical Program, Expanded Abstracts, pp. 1188-1191.

Eaton, D.W., Stewart, R.R. and Harrison, M.P. [1991] The Fresnel zone for P-SV waves. Geophysics, 56(3), pp.360-364.

JafarGandomi, A., Richardson, J., Hoeber, H., Galyga, M., Smith, P. and Irving, A. [2018] Improved Reservoir Imaging Using Specular Dip-angle Migration. In 80th EAGE Conference and Exhibition, Extended Abstracts, A15-20.

Tabti, H., Gelius, L.J. and Hellmann, T. [2004] Fresnel aperture prestack depth migration. First Break, 22(3), p.39-46.

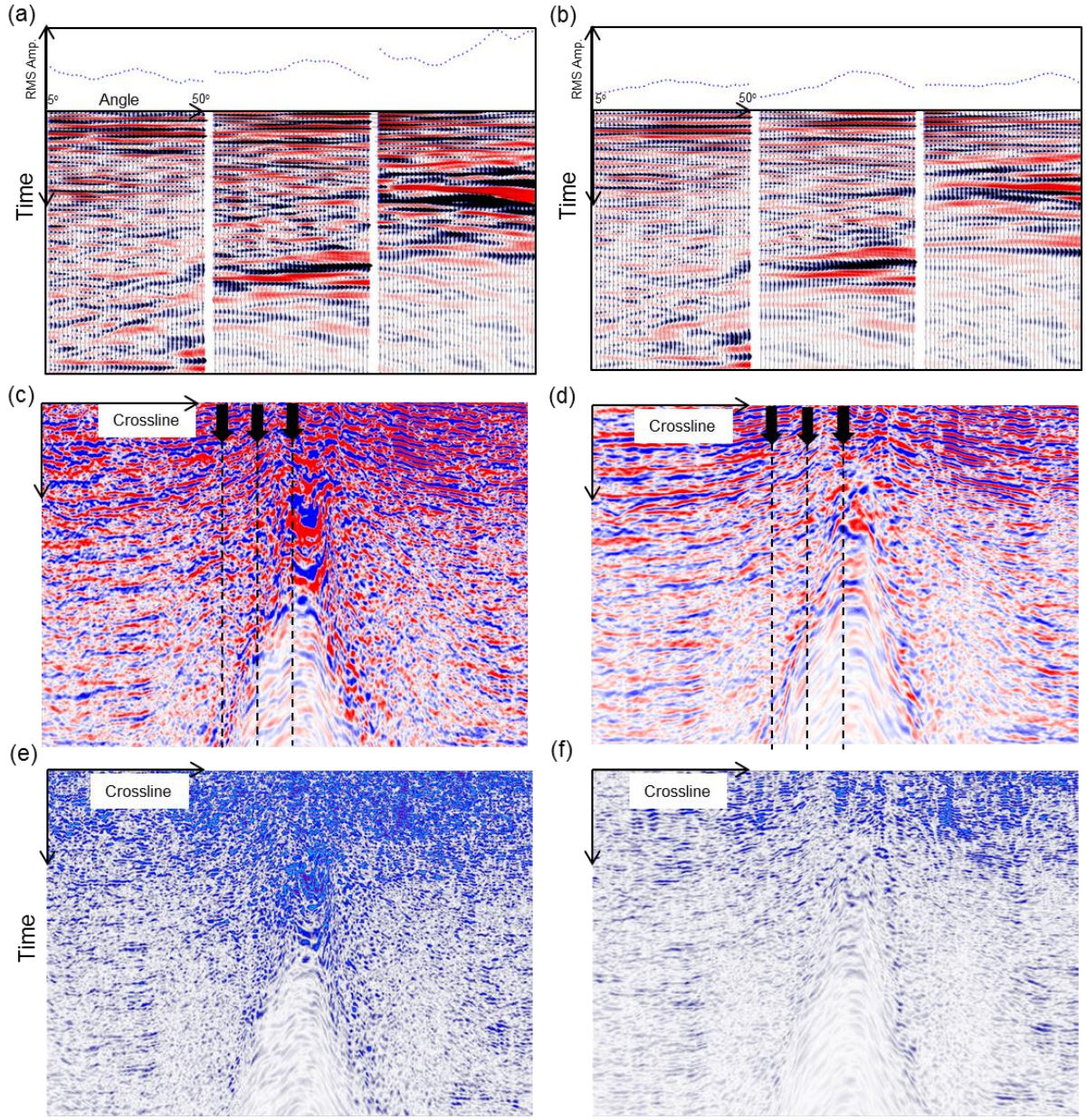

Figure 4 *Selected PS angle gathers and estimated PS AVO gradients for conventional (a & c) and specular (b & d) Kirchhoff PSDM. Black arrows indicate the locations of the selected gathers. Absolute values of PS AVO fit residuals (averaged over incidence angles 0-30) for (e) conventional and (f) specular Kirchhoff PSDM. Blue colour indicates higher value.*